



## Article

\*These authors contributed equally to this work.

**Cite this article:** Mallett R, Nandan V, Stroeve J, Willatt R, Saha M, Yackel J, Veysi re G, Wilkinson J (2024). Dye tracing of upward brine migration in snow. *Annals of Glaciology* 1–14. <https://doi.org/10.1017/aog.2024.27>

Received: 21 December 2023

Revised: 7 June 2024

Accepted: 30 June 2024

**Keywords:**





sea ice; snow; snow physics

**Corresponding author:**

Robbie Mallett;

Email: [robbie.d.mallett@uit.no](mailto:robbie.d.mallett@uit.no)

## Dye tracing of upward brine migration in snow

Robbie Mallett<sup>1,2,3,\*</sup> , Vishnu Nandan<sup>1,4,5,6,\*</sup>, Julianne Stroeve<sup>1,3,7</sup> ,  
Rosemary Willatt<sup>3,8</sup>, Monojit Saha<sup>1</sup>, John Yackel<sup>4</sup>, Ga lle Veysi re<sup>3,9</sup>  and  
Jeremy Wilkinson<sup>9</sup> 

<sup>1</sup>Centre for Earth Observation Science, University of Manitoba, Winnipeg, Canada; <sup>2</sup>Earth Observation Group, Department of Physics and Technology, UiT The Arctic University of Norway, Norway; <sup>3</sup>Centre for Polar Observation and Modelling, Department of Earth Sciences, University College London, London, UK; <sup>4</sup>Cryosphere Climate Research Group, Department of Geography, University of Calgary, Calgary, Canada; <sup>5</sup>H2O Geomatics Inc, Kitchener, Ontario, Canada; <sup>6</sup>Department of Electronics and Communication Engineering, Amrita University, Kollam, India; <sup>7</sup>National Snow and Ice Data Center, University of Colorado, Boulder, CO, USA; <sup>8</sup>Centre for Polar Observation and Modelling, Department of Geography and Environmental Sciences, University of Northumbria, UK and <sup>9</sup>British Antarctic Survey, Cambridge, UK

**Abstract**

Salt is often present in the snow overlying seasonal sea ice, and has profound thermodynamic and electromagnetic effects. However, its provenance and behaviour within the snow remain uncertain. We describe two investigations tracing upward brine movement in snow: one conducted in the laboratory and one in the field. The laboratory experiments involved the addition of dyed brine to the base of terrestrial snow samples, with subsequent wicking being measured. Our field experiment involved dye being added directly (without brine) to bare sea-ice and lake ice surfaces, with snow then accumulating on top over several days. On the sea ice, the dye migrated upwards into the snow by up to 5 cm as the snow's basal layer became more salty, whereas no migration occurred in our control experiment over non-saline lake ice. This occurred in relatively dry snowpacks where brine took up < 6% of the snow's calculated pore volume, suggesting pore saturation is not required for upward salt transport. Our results highlight the potential role of microstructural parameters beyond those currently retrievable with penetrometry, and the potential value of longitudinal, process-based field studies of young snowpacks.

**1. Introduction**

Sea ice in both polar regions is becoming increasingly seasonal due to the decreasing area of sea ice which survives each summer melt season (Stroeve and Notz, 2018; Babb and others, 2023). The snow on the increasing fraction of first-year ice (FYI) is geophysically distinct from that on the decreasing fraction of multi-year ice because of its characteristic salinity. Snow salinity on FYI can reach upwards of ten parts per thousand in the basal snow layers (Nandan and others, 2017). The presence of such a quantity of salt modifies the thermodynamic and electromagnetic properties of the snow, which in turn affect its geophysical evolution (e.g. Crocker, 1984). Alteration of the snow's dielectric properties impact active and passive microwave remote sensing (Barber and others, 1998; Nandan and others, 2020).

Despite its importance, the source and pathways that deliver salt into the snow are still poorly understood; potential mechanisms range from deposition of salt-aerosols from nearby open water areas, wind-driven redistribution of snow grains that have saltated over newly formed sea ice, and upward capillary action from newly forming ice (Perovich and Richter-Menge, 1994; Domin  and others, 2004). This complexity has so far prevented Arctic Ocean snow models such as SnowModel-LG (Liston and others, 2020) and NESOSIM (Petty and others, 2018) from including salt-related processes in their modelled snowpacks. Wever and others (2020) recently adapted the one-dimensional SNOWPACK snow model for the sea-ice environment. It is now capable of simulating flooding of the snow from negative ice freeboard, and has a sophisticated scheme for handling downward percolation of water based on its parameterisation of snow microstructure. However, it has not yet clearly exhibited upward movement of brine into the snow from capillary pressure, or reproduced the typical vertical profiles of snow salinity observed in situ. If any of the models mentioned above are to accurately reproduce these profiles then the real-world processes that produce them must first be characterised. Here we use dye-tracing for tracking the upward movement of brine in both the laboratory and field-based experiments.

**1.1. The nature and importance of snow salinity**

Fresh (used here to mean non-saline) snow has a melting point of 0 C. While microscopic quasi-liquid layers do exist on the surface of snow grains below that temperature (Sazaki and others, 2012), a fresh snowpack does not exhibit liquid water in quantities relevant to most thermodynamic or electromagnetic considerations below 0 C. When salt is introduced to the snowpack in limited quantities, the physics of the system is changed from a two-phase (air/ice) system to a three-phase system (air/ice/brine), and this excludes the complication of

  The Author(s), 2024. Published by Cambridge University Press on behalf of International Glaciological Society. This is an Open Access article, distributed under the terms of the Creative Commons Attribution licence (<http://creativecommons.org/licenses/by/4.0/>), which permits unrestricted re-use, distribution and reproduction, provided the original article is properly cited.

[cambridge.org/aog](https://www.cambridge.org/aog)



salt precipitating out of the brine to create a fourth mixture component (see Butler and others, 2016, for this precipitation in sea ice itself). Put simply, the presence of salt in snow allows saline liquid water (brine) to coexist in a phase equilibrium with the ice lattice at sub-zero temperatures (Stogryn, 1986; Geldsetzer and others, 2009).

Water is an excellent conductor of heat relative to ice and air, and so the thermal conductivity of the ice/air/water mixture is increased (Crocker, 1984). Furthermore, water is an excellent absorber of microwaves relative to ice and air (Drinkwater and Crocker, 1988); this reduces the ability of microwaves to penetrate the saline snowpack on FYI. This effects coherent microwaves transmitted from and backscattered to radars such as altimeters and scatterometers (Barber and Nghiem, 1999; Nandan and others, 2016, 2017; Yackel and others, 2019; Nandan and others, 2020), but also natural microwave emission from the snow-covered ice surface as measured by radiometers (e.g. Barber and others, 1998, 2003; Markus and others, 2009).

The presence of salt within snow-covered sea ice also affects the lower atmosphere. As well as being photochemically relevant (Dominé and Shepson, 2002; Wren and others, 2013), saline snow produces salt aerosols when redistributed by wind (Frey and others, 2020; Confer and others, 2023). This can nucleate clouds, in turn modifying the radiative balance of the atmospheric boundary layer (Gong and others, 2023).

### 1.2. Potential mechanisms for production of saline snow over first-year ice

The processes that dictate the timing and extent of snow salinification over sea ice are not well understood (Dominé and others, 2004). This is in part because the snow cover on sea ice is frequently redistributed by the wind, making a single vertical column of snow (like that represented by a 1-D model such as Wever and others (2020)) both difficult to observe continuously and often not representative of heavily redistributed snow on an ice floe.

Dominé and others (2004) discuss three main potential mechanisms of salinification: deposition from above by either (1) wind-blown frost flowers, (2) sea salt aerosol generated by sea spray or (3) transport from the ice below via capillary forces. Here, we focus on the contribution from the latter mechanism of upward wicking via capillary action, and this requires the presence of brine at the base of the snowpack. There are two typical routes that deliver brine to this location. One involves the presence of a thin layer of brine that is deposited on the sea-ice surface during its formation, described as a brine *skim* by Perovich and Richter-Menge (1994). This might be upwardly rejected during nilas formation or the consolidation of frazil ice, or might be left on the ice surface having spilled over the side of a piece of pancake ice due to wave action. While the skim may mostly freeze as the ice thickens and its upper surface cools, falling snow will increase the skim's volume by providing thermal insulation from the cold air. If it has sufficient volume, brine from the skim can then potentially migrate upwards in the snow via capillary action. In this case, moisture is scarce, and we suggest the height of wicking will likely be limited by the brine supply simply running out.

Another mode of brine delivery to the base of the snowpack is flooding of the ice surface (e.g. Provost and others, 2017). This occurs when so much snow accumulates that it presses the ice below the waterline. In this case, the brine supply is often abundant, and the height of subsequent wicking will likely be limited by the ability of the snow microstructure to sustain the surface tension required to hold the liquid up against gravity. A photo of the phenomenon is given in Figure 2 of Willatt and others

(2010), and we also include a higher resolution colour photo of the phenomenon in Supplementary Figure S1. This phenomenon was visualised by Massom and others (2001, see their Figure 6) by introducing dyed brine to the base of an Antarctic snow sample and photographing the result shortly afterwards.

Here, we present a series of experiments following Massom and others (2001) which investigate the potential of coloured dye to trace the upwards migration of brine both instantaneously and over time. We begin by detailing laboratory-based investigations where dyed brine is introduced at the base of terrestrial snow samples, and the brine transport is visibly traced upwards. By introducing brine, we mimic flooding of the base of the snow and subsequent wicking above the waterline. We then show how this technique can also be used in a real sea-ice environment with a positive freeboard: we show results of a pilot study on land-fast FYI and lake ice in Hudson Bay, Canada. In this case, we suggest the wicking can be attributed to what remains of a brine skim. Finally, we reflect on the shortcomings of both experiments, and make suggestions for future research directions.

## 2. Methods

### 2.1. Dye selection

We use a Rhodamine-WT dye to trace the migration of brine from the snow/sea-ice interface. This fluorescent, pink dye has a freezing point of 0°C and a specific gravity of 1020 kg m<sup>-3</sup> (at 25°C). Compared to other water tracing dyes, it has a relatively low cost and has a low minimum detectability (Smart and Laidlaw, 1977; Davis and Dozier, 1984). It also has the advantage of having a similar density to brine, and having the same freezing point as pure water. The latter characteristic means that where salt does not exist, the dye will not alter the properties of the water itself, nor melt snow in areas where no liquid exists. We manually verified that the addition of the dye to water does not alter its conductivity as measured by an Oakton CON 450 conductivity meter, which was used for all field-based salinity analysis.

At this point, we point out four other studies that have used tracer dyes to study *downward* liquid movement in the sea-ice context, in addition to Massom and others (2001) which was mentioned in our introduction. Nicolaus and others (2009) used Sulforhodamin-B (SB) to trace the downward percolation of snow meltwater in the spring–summer transition in the Weddell Sea. We elected not to use SB due to its hydrophilic properties, which were raised by the authors in their study. SB was also used alongside fluorescein by Freitag and Eicken (2003) to study sea-ice permeability to meltwater, following Eide and Martin (1975) who used thymol-blue and Bennington (1967) who used a proprietary dye named Dy-Chek designed for automobile inspections.

### 2.2. Rothera laboratory experiments

We performed two rounds of laboratory experiments each lasting 9 d at Rothera research station in West Antarctica during August and October 2023. In each round, we identified two distinct stratigraphic layers in nearby terrestrial snow that would allow us to take ten similar snow samples from each layer. We produced 20 labelled polyvinylchloride (PVC) tubes (19 cm long, 6.4 cm internal diameter) which could be driven into our chosen snow layers horizontally, and then extracted with a snow sample inside (Fig. 1a). This allowed us to extract several internally homogenous cylindrical snow samples of similar snow properties upon which we could experiment. It would have been preferable to sample the snow with the tubes orientated vertically, but the available snow stratigraphy did not include layers thick enough to ensure

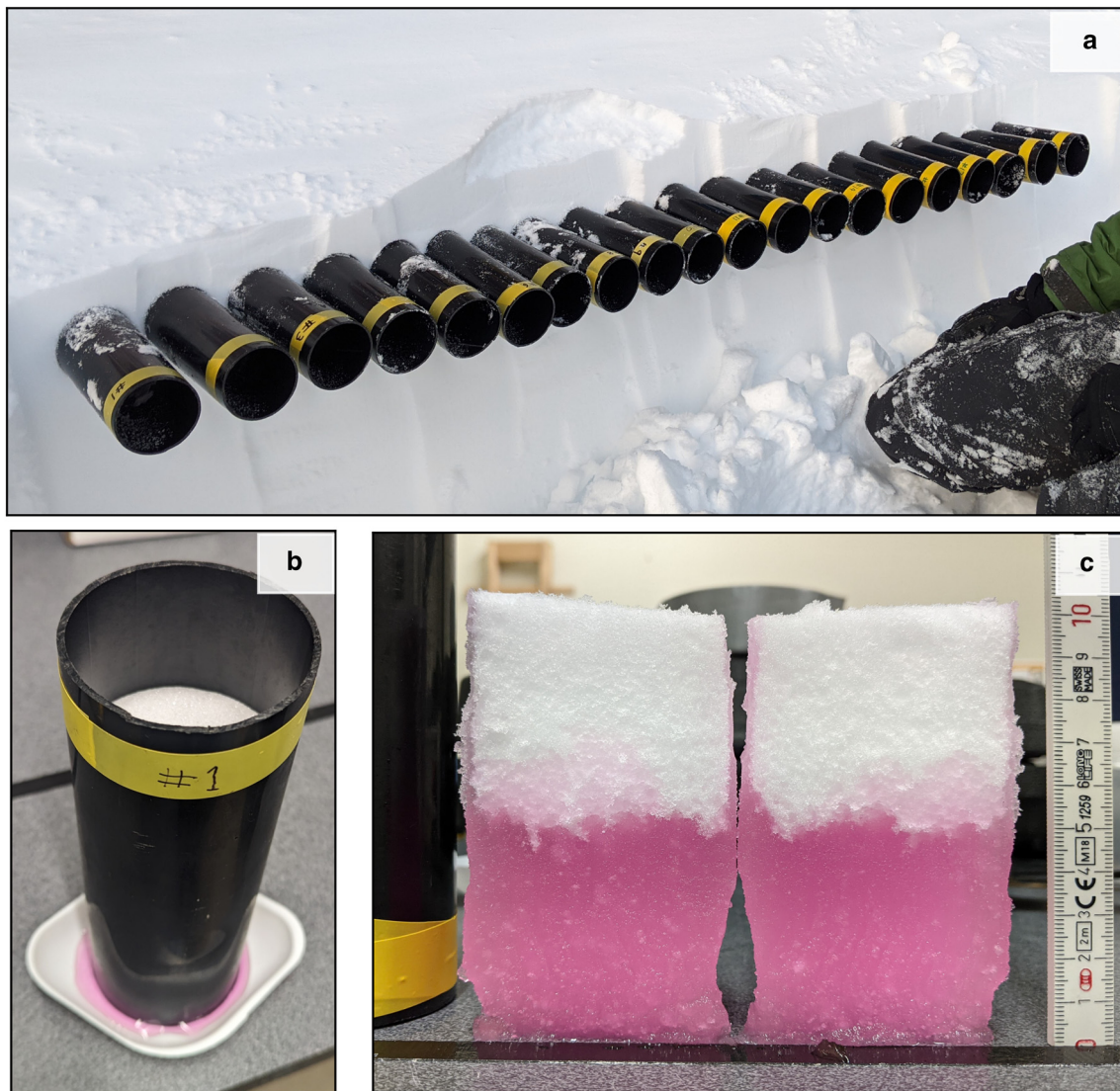


**Figure 1.** Photographs showing the experimental procedure. (a) 19 cm plastic tubes were driven into a coherent layer of snow such that they each contained a sample with similar snow properties. In this photo the tubes are protruding from the wall of the snow pit. To sample the snow, they were pushed all the way in and then dug out by hand. (b) Snow samples were then taken to the laboratory, where they were brought to a consistent temperature and then dyed brine was added to the base. Photograph shows the sample after several days: the snow surface has sunk within the tube, and the sample has begun to reject some brine back into the weighing boat. (c) At the end of the experiment, samples were removed from the tubes, dissected and photographed against a ruler. Geophysical sampling was then performed on the sample.

that snow properties would be uniform throughout the 19 cm long tube. Layers were however thick enough to allow horizontal sampling, with the 6.4 cm tube diameter being small enough to allow the tube to be entirely contained within a distinct, homogeneous snow layer when horizontal. Attempts were made to measure the internal stratigraphy of snow samples using a snow micropenetrometer: unfortunately the geometry of the sampling tube and the conical tip of the rod led to snow being pushed up against the edges, which led to large measurement errors. In future, micro-CT analysis may shed light on the internal stratigraphy of a given set of samples. We cooled the plastic tubes in nearby snow before inserting them into the layers such that their temperature matched the samples as the tubes were driven in. While establishing our protocol, we found that not cooling the tubes led to the snow sample adhering to the sides and behaving erratically during the experiment. After the samples were extracted from their respective layers, we took manual density measurements of the layers using a 250 cm<sup>3</sup> cylindrical snow cutter with a 5 cm internal diameter. We also separately measured the layers in situ with the snow micropenetrometer (v4

Schneebeli and Johnson, 1998) to estimate the density and specific surface area (SSA) of the snow using the method and coefficients of Proksch and others (2015a).

Once the snow samples were brought into the lab, they were left in the freezer at  $\sim -5.6^{\circ}\text{C}$  for at least 1 h. This allowed them to come to a common temperature with each other before having brine added, but also produced a consistency of treatment between rounds. Because of its gas-based thermostat, the freezer that hosted our experiments underwent thermal cycling where the compressor would periodically switch on and off. To investigate the impact of such a cycle, we created a dummy sample where a digital temperature logger was encased in snow during the second round of the experiments in October. The logged temperatures are shown in Supplementary Figure S2, and had a mean value of  $-5.61^{\circ}\text{C}$  and a standard deviation of  $0.22^{\circ}\text{C}$  in the 9 d period for which the dummy sample was present in the freezer alongside the main experiment.

Samples were seated in 100 ml plastic weighing boats, visible in white at the base of the sample in Figure 1b. This allowed the same amount of brine to be consistently supplied to the base of

each sample. Earlier attempts at the experiments saw several samples seated in the same tray, and brine added to the tray (Supplementary Fig. S3). Because of small inconsistencies in the sample extraction procedure or the cutting of the plastic tubes, the ‘one tray’ approach led to some samples taking up the brine faster than others, leading to inconsistent handling of different samples within the same round. In the final iteration of our experiments (presented here), 50 ml of brine was added rapidly to each sample successively. We discuss the salinity of the brine below. Samples took up all the brine within a few seconds; we provide a video (Supplementary Video S1) of this immediate uptake using a special setup where the PVC tube is suspended with a clamp stand to improve visibility.

To make our experiments as easy to interpret as possible, we chilled the dyed brine to the temperature of the snow by storing it in the freezer where the snow samples equilibrated. Adding the brine at the temperature of the snow ensured that there was no exchange of sensible heat between the brine and the snow upon addition. The decision to do this influenced our choice of brine salinity: the brine must reliably not freeze while in storage (even partially), but it also must not be so saline that salt would precipitate out in storage. For example, using simple dyed seawater would have resulted in the formation of sea ice at the temperature of the freezer, but 500 parts of salt added to a thousand parts water would not dissolve completely. To ensure we selected an appropriate salinity, we considered the phase function of seawater brine near its freezing point (Figure 1 of Weeks, 1968). Following Equation 1c from Frankenstein and Garner (1967), the equilibrium brine salinity ( $S_b$ ) in parts per thousand (ppt) at a given temperature ( $T$ ) in degrees Celsius ( $^{\circ}\text{C}$ ) can be described:

$$S_b = \frac{T}{T - 54.11} \quad (1)$$

Our dummy sample indicated that the freezer was operating at a mean temperature  $-5.61^{\circ}\text{C}$ , with a corresponding equilibrium salinity ( $S_b$ ) of 94 ppt. We therefore selected a brine salinity of 100 ppt to ensure that there would be no partial freezing of the brine in storage.

Because of the way the tubes were inserted into the snow layers, the snow adjacent to the plastic likely experienced friction and compression. This led to edge-effects which meant it was not possible to observe the height of internal brine wicking by looking at the snow sample from the outside, even when the plastic tube was removed. Samples therefore had to be dissected with a snow scraper and viewed in cross section for the wicking height to be reliably established. Figure 1c shows a sample’s dissected cross section, as well as the edge effects that run vertically up the sides of the samples.

Once dissected, the sample’s cross section was photographed alongside a ruler. The camera was placed at a consistent distance from the samples such that photos are intercomparable. The height to which the snow was dyed was not always horizontally consistent. To generate a single, indicative height value for inter-comparison between samples, the maximum and minimum wicked height in a sample were horizontally referenced to the ruler (to the nearest millimetre), and then averaged. The height of wicking at the sample edges was not considered when characterising the maximum height due to the edge effects discussed above.

Two stratigraphic layers were sampled in each round, with the two rounds of sampling occurring on the 21st of August and the 5th of October. We had 20 sampling tubes, so allocated ten to each layer in each round (thus sampling four layers over the two rounds). For each round, we sampled what at the time were subjectively observed to be a hard snow layer and a soft snow

layer. Henceforth, these layers will be referred to as August Soft, August Hard, October Soft and October Hard. After the addition of dyed brine, eight of the ten samples from a layer were placed in the freezer. In round one, the remaining two samples from each layer were immediately dissected and the initial wicking height was characterised – they were found to be similar. This similarity led to only one sample being immediately dissected in round two. This made an additional snow sample available for each of the layers in round two, which we elected to not add brine to. Instead we monitored the degree to which the sample settled in the tube in the absence of brine addition, for later comparison with the measured sinking of the samples with brine in them. A schematic of the sample allocation is given in Supplementary Figure S4.

The experiment was conducted over nine days: the period was determined by monitoring the rate at which the upper snow surfaces of the samples were sinking. A judgment was made during the first (August) round of experiments that this had effectively stopped after nine days, with any residual sinking potentially being attributable to natural settling processes (i.e. dry snow metamorphism) not involving the brine itself. Prior testing and development of the laboratory procedure also indicated that wicked heights did not clearly increase beyond this timescale.

By the end of the nine day experiment, the upper snow surfaces of samples to which brine had been added had sunk by several centimetres in their tubes, and had released dyed brine back out into the weighing boat, which began to freeze over by the end of the experiment. This is visible in Figure 1b: the snow originally filled the black tube to the top, and a halo of pink released brine has appeared around the bottom of the tube in the weighing boat. The partially frozen released brine was weighed, brought to room temperature and its salinity then was measured. Because the distance by which the snow surface had sunk could be measured non-destructively, this was recorded every day. When each sample was eventually dissected and the wicking height was measured, the salinity of its bottommost 3 cm layers was also recorded (0–3, 3–6 cm). All salinity measurements were taken using a Thermo Scientific Orion Star A221.

### 2.3. Churchill field experiments

Our field study was performed on newly formed sea and lake ice near Churchill in the Western Hudson Bay of Canada during December 2021. By the time we were able to access the sea ice with the dye, a thin snow cover of  $\sim 5$  cm had already accumulated. This posed the problem of how the dye could be supplied to the base of the snowpack. We cleared a patch of sea ice by gently clearing the snow using a shovel and then a stiff-bristled brush, aiming to minimally disturb the ice surface. We then applied the dye to the ice surface in its neat form, without mixing it with brine as in the lab experiments. We then hypothesised that the subsequent snow accumulation (from fresh snowfall and blowing snow) would insulate the ice surface, such that a liquid phase would emerge, mix with the dye and wick up into the snow.

At the first site on the 4th December (Dye Pit 1; DP1) we applied the dye directly from the bottle in a line on the ice surface (Fig. 2a). This was to help characterise lateral migration of the dye, as well as vertical. At the second (DP2;  $\sim 10$  m away) on the 9th December, it was sprayed over an area approximately  $0.3 \times 1$  m from a spray bottle (Fig. 2b). This was motivated by more even dye application, with the potential to better characterise the horizontal variability of the vertical brine migration – unfortunately this did not transpire and the spray-gun gave a somewhat patchy application. After dyeing the ice surfaces, snow was allowed to accumulate over several days. The sites were then revisited

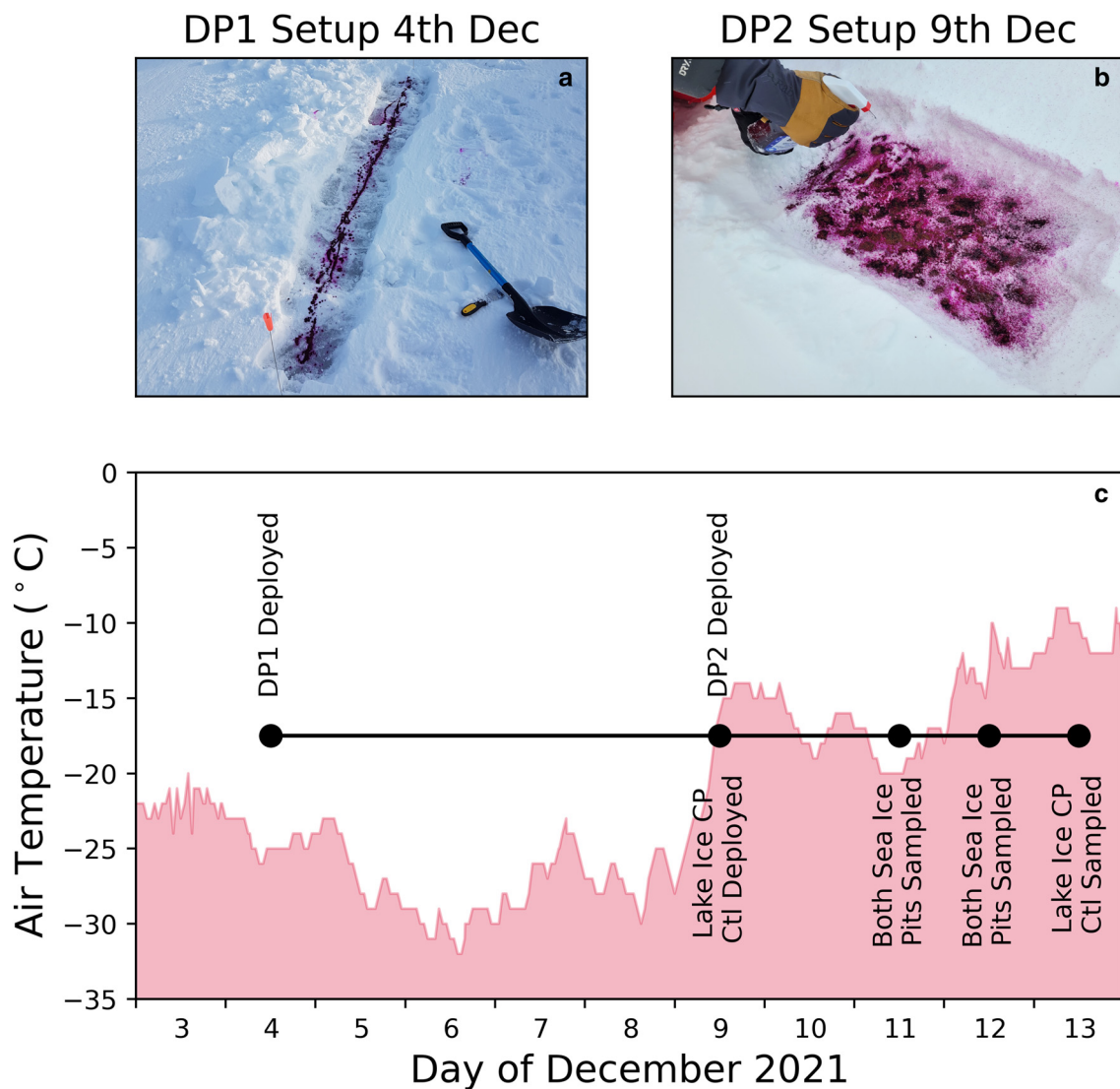


**Figure 2.** (a) The setup of DP1, where dye was applied 'neat' from the bottle in a line onto the sea-ice surface after snow clearing. This was to help characterise horizontal migration. (b) Setup of DP2, where dye was more evenly applied over an area with a spray bottle. (c) Timeline of the deployment and sampling of the three sites described in this manuscript: DP1, DP2, CP. The red-shaded timeseries indicates the air temperature recorded hourly at the Churchill airport 15.5 km to the west-south-west of the sea-ice sites. Air temperatures measured at the airport were consistently below  $-10^{\circ}\text{C}$  for the duration of the sea-ice experiment.

throughout the campaign (see Fig. 2c for timeline), with a snow pit dug at each site at each visit (DP1 and DP2). On the 4th December (when DP1 was set up), the ice thickness at the site was measured to be 33 cm thick, with a freeboard of 2 cm.

We also set up a control experiment (Control Pit; CP) on nearby lake ice, with dye applied via spray-gun in a similar fashion to DP2 on the sea ice. The dye was applied on the 9th December, on the same day as DP2. Both the sea-ice and lake ice sites were visited opportunistically, with a period of cold weather prior to the 9th of December (Fig. 2c) precluding access, and separate planned work as part of a wider radar-science campaign precluding access on the 10th. When the dye was deployed, the adjacent lake ice thickness was measured to be 67.5 cm, with a freeboard of 2.5 cm. This control experiment was designed to show that the dye does not possess some inherent wicking property independent of brine migration. If the dye at CP was seen to migrate up the snow without the presence of salt, then it would invalidate the dye as an experimental tool for monitoring brine dynamics. The control experiment was performed on a frozen lake 4.7 km south of the sea-ice sites DP1 and DP2. At both the beginning and the end of the experiment snow and ice salinities were measured to be  $<0.02$  ppt. This is more than an

order of magnitude smaller than the lowest salinity recorded at the sea-ice sites, and approaching the resolution of the salinity meter stated by the manufacturer (0.01 ppt; Industrial Process Measurement Inc, 2016). Supplementary Figure S5 shows the relative locations of the field sites. Prior to applying the dye, we took scrapings of the ice surface ( $\sim 5$  mm deep) to characterise its salinity. When we revisited the sites to measure the dye migration and dig snow pits, we measured the ice surface salinity, and the snow density, temperature and salinity at 2 cm vertical intervals. We measured the height of dye migration with a ruler, and took photographs. At DP1, where the dye was applied in a line (Fig. 2a), we measured the dye migration height directly above the line along which the dye was applied (Figs 8a–c). For DP2 (where the dye was distributed with a spray-gun, Fig. 2b), we took the average of the minimum and maximum height to which the dye had migrated over the region in which it was applied (Figs 8d,e), similar to the laboratory measurement protocol. We note that the dye migration height was recorded in the field, rather than extracted from the photos shown in Figure 8. Snow density was measured with a  $66\text{ cm}^3$  density cutter which allowed layer-wise sampling with a vertical resolution of 2 cm.

### 3. Results

#### 3.1. Rothera laboratory experiments

The snow micropenetrator measurements indicated that the hard and the soft layers sampled in both August and October were geophysically distinct with regard to retrieved density and SSA (Fig. 3). The soft snow sampled in October had properties that departed the most from the other three, both in terms of density and SSA. The SMP's density retrievals consistently overestimated that which we measured with our 250 cc density cutter. Evidence from Proksch and others (2016) indicates that the cylindrical cutter itself may underestimate or overestimate low and high densities respectively compared to relatively accurate micro-CT analysis. However, the magnitudes of these biases are considerably smaller than those seen here relative to the SMP, and so we consider the density cutter results more reliable. One key feature of the data is that while there does appear to be an offset between the cutter-based and SMP-based densities, the August Hard and October Soft layers are the most and least dense when measured through both methods. This suggests that while the magnitude of the density-based effects here may contain a bias stemming from measurement-related uncertainty, the sign of the relationships will likely be robust.

In Figure 3 we only show data from the first 30 mm of probe penetration, despite collecting data over a relatively large probe penetration range. This is because snow in the upper levels of the layers was removed, so as to be certain that the first snow encountered by the probe was from the layer that provided the snow samples to the brine wicking experiment. So while the first few centimetres of SMP data are consistently reliable, the probe in some cases then encountered the layer below which was not sampled and so is not relevant to our investigation and not shown here.

All four of the snow layers' samples immediately soaked up all the 50 ml of 100 ppt brine that was applied (see Supplementary Video 1). In our first experimental round, we immediately dissected two samples from each of the two layers. Their cross sections revealed that the brine had wicked to a height of around 3.5 cm for both the hard and the soft snow. In the second round, we incorporated two control samples where brine was not added, so only cut one sample from each layer open initially. The heights were 2.2 cm for both the hard and the soft snow.

After waiting nine days, the height to which dye was present increased across all four snow layers. As a percent of the initial height reached, the 10-day heights were 153, 150, 131 and 204% for samples 1–4 respectively (5.5, 5.2, 2.9, 4.5 cm total height, on average). A clear relationship between wicking heights and the density/SSA measurements is not evident (Fig. 4). However, it is clear that the sample with the lowest density (and highest SSA) did wick substantially less than the other samples.

While the dye ascended into the snow samples over time, it also appeared to be a much less vivid shade of pink. This is consistent with significant dilution of the dyed brine solution. We validated this with bulk salinity measurements of the samples' bottom 3 cm. The bottom 3 cm of layers 1–4 exhibited the following initial bulk salinity values: 61.3, 61.2, 58.5 and 67.1 ppt. These values are relative to the salinity of the initially added brine of 100 ppt. After 10 d, the average bulk salinity in the same 0–3 cm section of the samples was depleted to average values of 28.9, 35.7, 47.5 and 38.1 ppt. The basal bulk salinity of the samples was inversely correlated with the height to which the dye wicked (Fig. 5b;  $r = 0.92$ , slope =  $-6.1$  ppt per cm of wicked height).

The reduction in the basal bulk salinity over the 9 d period indicates that there is less salt by weight in the bottom three centimetres of the sample. So where does the salt go? One pathway is up: the brine travels further up into the sample, out of the 0–3 cm

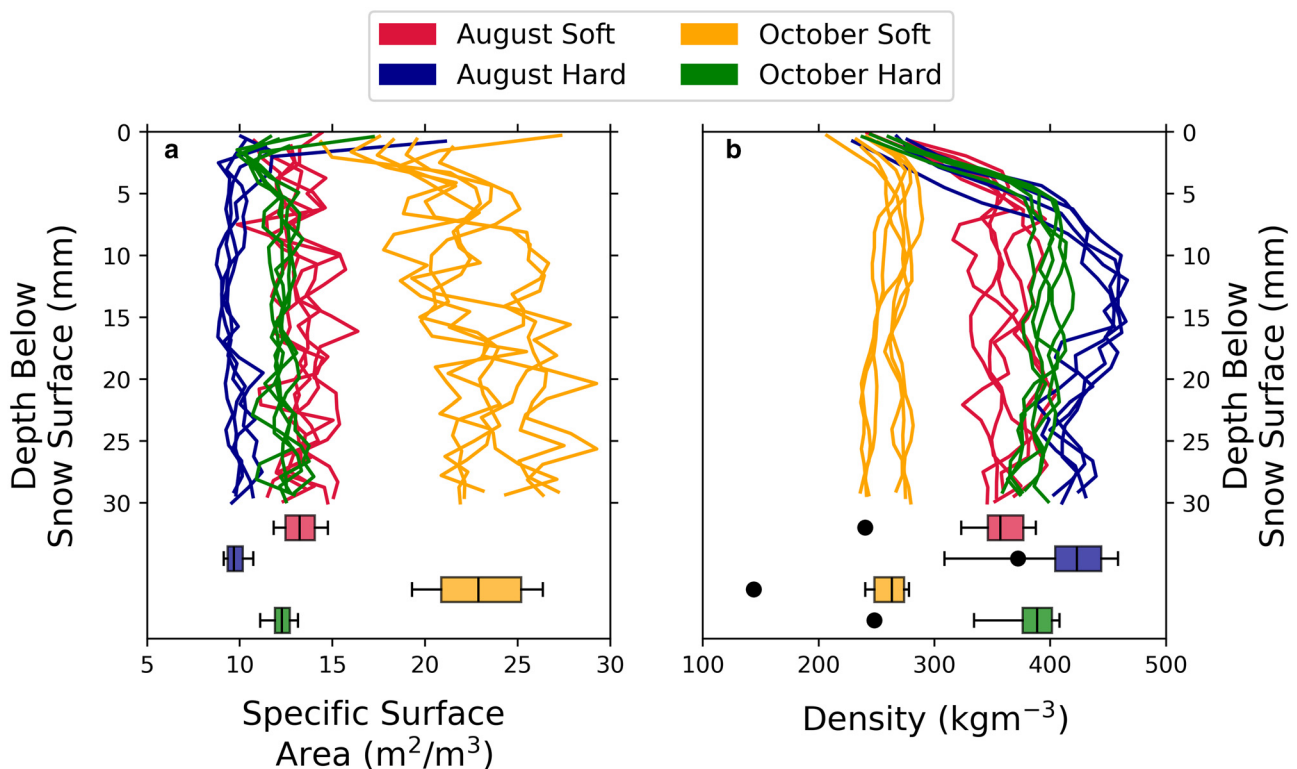


**Figure 3.** (a) Specific surface area and (b) density from the four snow layers sampled over the first 30 mm of probe penetration. Line plots indicate the SSA/density retrievals based on the parameterisation of Proksch and others (2015b). Box plots indicate the distribution of data from all five samples of each layer over the 30 mm range. Whiskers of the box plots indicate the 10th and 90th percentile, horizontal central lines indicate means. Round markers in panel (b) indicate the mean of the three manual density measurements performed on each layer with the 250 cc cylinder.

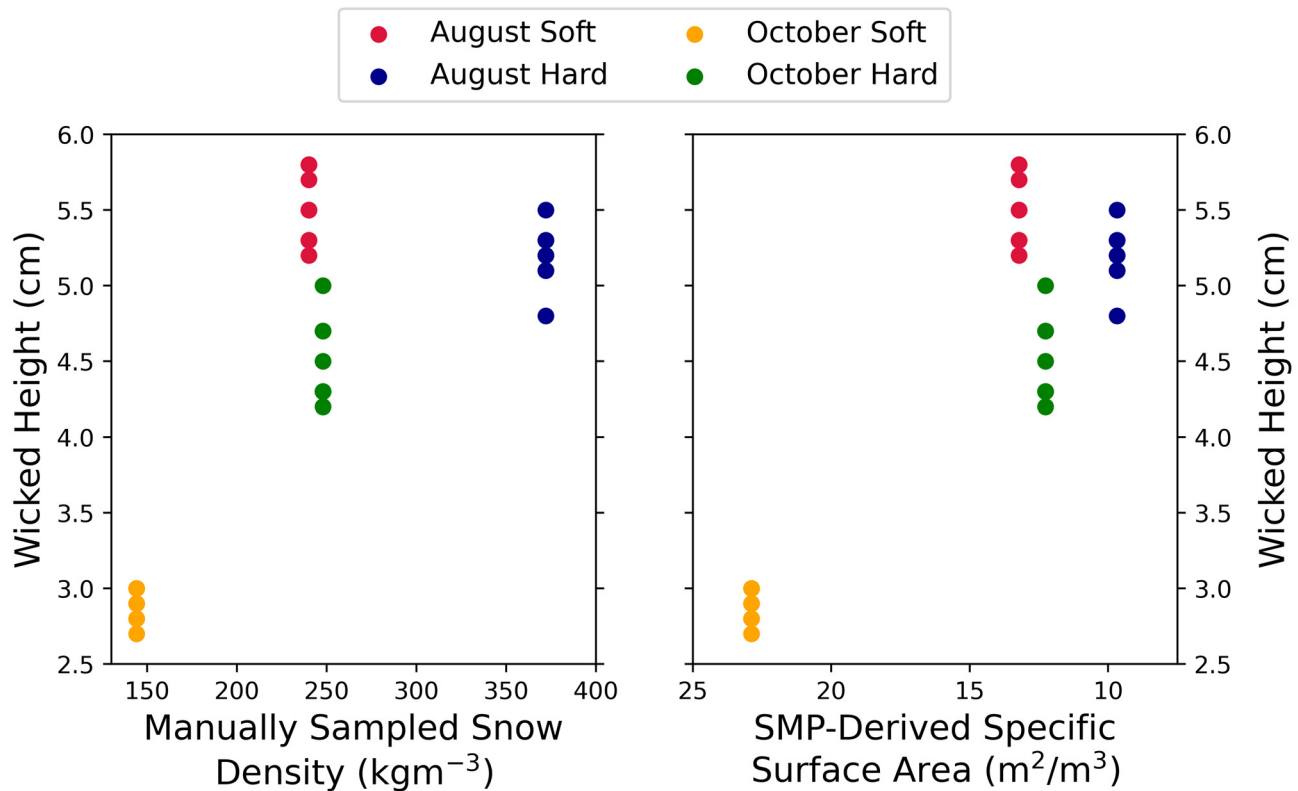


**Figure 4.** Height to which dyed brine wicked in snow samples, shown as a function of snow density and estimated specific surface area. Samples displayed with a single x-coordinate based on the mean of in situ measurements of the snow layer from which they were taken.

basal layer to heights above. This explains the strong correlation between wicked height and basal bulk salinity. However, another potential pathway is downwards: we observed the release of dyed brine from the base of the samples several days after the brine was initially added. The released brine was weighed and its salinity was measured. The mean values of the four layers were 65.6, 57.5, 70.9 and 68.4 ppt, and the corresponding weights were 58.8, 20.2, 27.37 and 15.74 g. The salinity of the released brine was therefore much more saline but also well correlated with the basal bulk salinity (Fig. 5a;  $r = 0.85$ , slope = 1.05 ppt of salinity in the released brine for every 1 ppt of salinity in the basal bulk snow). We will later discuss to what degree the salinity of the released brine might reflect the salinity of the liquid phase in the bulk snow volume above.

We finally turn to the timescale on which the brine migrates up into the snow after it is initially absorbed. We took daily measurements of the height by which the snow surface had sunk relative to the top of its PVC tube, and show the results in Figure 6. Figure 6 illustrates that many of the samples initially adhered to the sides of the tubes, and thus did not sink immediately. This was particularly the case for the experiments in October. The data on sinking rates also show that many of the samples were still sinking at the end of our 9 d experiment. This appears to particularly be the case with October's soft layer, where the top of the snow samples had sunk by an average of 7 mm on the final day of the experiment. If we assume that a sample's sinking rate corresponds to the wicking rate, the fact that October's soft samples were still sinking when dissected may explain why the wicking heights were so much lower than for the soft snow in August (Fig. 4). We do not have an obvious explanation for why the October soft snow samples were so much slower to wick and sink than in August, however we do point out that the density and derived SSA of the samples was much lower (Fig. 4).

We have avoided describing the sinking of the brine-wetted snow as *settling* here because the brine might make the process

quite different from the settling of dry snow (see Bernard and others, 2023, for a recent summary). We investigated this difference during the second round of our experiments by monitoring the 'control' settling rate of dry snow samples that were left brine-free (dashed lines in Fig. 6). This could then be compared to the rate at which the brine-wetted samples from the same snow layers sank. Settlement of the dry snow samples is shown by dashed lines in Fig. 6. At the end of the October experiment the soft and hard dry snow samples had settled by 1.8 and 0.8 cm respectively (9.4 and 4.2% of the initial 19 cm sample height). For comparison, the mean sinking of the soft and hard samples with brine were 6.3 and 4.5 cm respectively (33 and 24%). This supports the notion that significant microstructural reconfiguration is attributable to the brine, causing faster sinking than the dry-snow settling rate.

### 3.2. Churchill field experiments

The two sea-ice sites (DP1 and DP2) had considerably different basal snow salinities. While both have decreasing snow salinities with height on all days that the accumulated snow was characterised, on the dates when both sites had the basal snow salinity (<4 cm) measured, the results showed salinity at DP1 was an order of magnitude larger than at DP2. This striking difference may be attributable to sea-ice dynamics during freeze-up: the exposed ice surface was noticeably rough, suggesting that the ice had not formed in situ under quiescent conditions but instead had potentially been driven into the bay (see Fig. S5) by tide or wind as small pieces before freezing up. This resulted in a rough ice surface with variable surface salinity.

We found the basal snow salinity at both pits increased with time (Fig. 7). At DP1 this is in contrast to the ice surface salinities underlying the snow pits, which decreased over time (not shown). The initial ice surface salinity at DP1 when the dye was deployed on 4th December was 15.12 ppt, and subsequently the ice surface

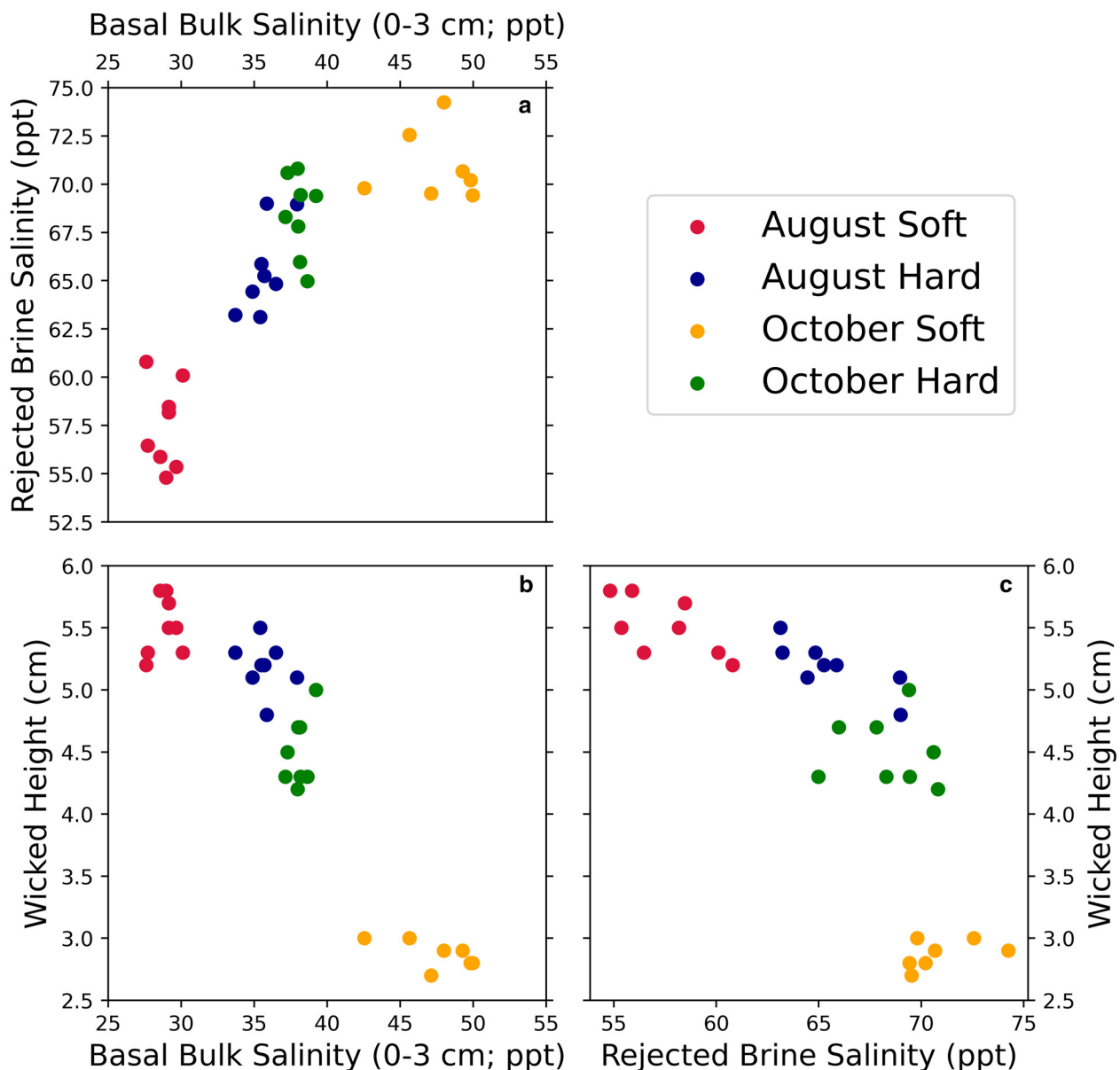


**Figure 5.** Relationships between wicked height, the bulk salinity of the sample's basal 3 cm and the brine that was released into the sample container. Clear relationships exist: a higher wicked height is associated with less salt in the base of the sample, and more diluted released brine. The experiment was begun by adding brine at an initial salinity of 100 ppt.

salinities were measured at 13.11, 10.25 and 6.5 ppt on the 9th, 11th and 12th of December. These measurements were taken in a similar fashion to the snow: samples were scraped into bags, then melted and analysed in the lab. As the ice underlying DP1 became fresher by 6.6 ppt, the snowpack base became saltier by 3 ppt. At DP2 the ice surface salinity was initially 4.85 ppt when the dye was applied on the 9th of December, and was subsequently 4.22 and 6.25 ppt on the 11th and 12th of December.

Because the dye at DP1 was deployed as a linear feature (Fig. 2a), we were able to observe what was significant lateral migration of the dye (visible in Figs 8a–c). From the photographs, it appears that the dye can migrate two or three times the distance laterally than it can vertically.

The lake ice control experiment (CP) was deployed on the same day as DP1, but observed on 2021-12-13, the day after the final measurements of the sea-ice pits. As such, the dye at the control site was allowed more time to migrate than either of the sea-ice based pits. Upon digging a snow pit, we observed no measurable upward migration. Snow and ice salinities from CP confirmed that both the snow and ice were fresh to within the

measurement accuracy of the instrument and method. We also observed while taking scrapings of the lake ice surface that the dye had not penetrated into the ice at all. However at the sea ice, the dye had penetrated at least 1 cm.

## 4. Discussion

### 4.1. Laboratory experiments

Based on our laboratory results, we now quantify what fraction of the snow samples' pore space might have been initially filled. The volumetric fraction of air in dry snow (sometimes called the porosity,  $P$ ) in a snow sample depends on its density (e.g. Essery and others, 2013):

$$P = 1 - \frac{\rho_s}{\rho_{\text{ice}}} \quad (2)$$

Where  $\rho_s$  is the specific gravity of the snow (i.e. the snow density as measured with our density cutter divided by the density of water), and  $\rho_{\text{ice}}$  is the density of pure ice which we take here to



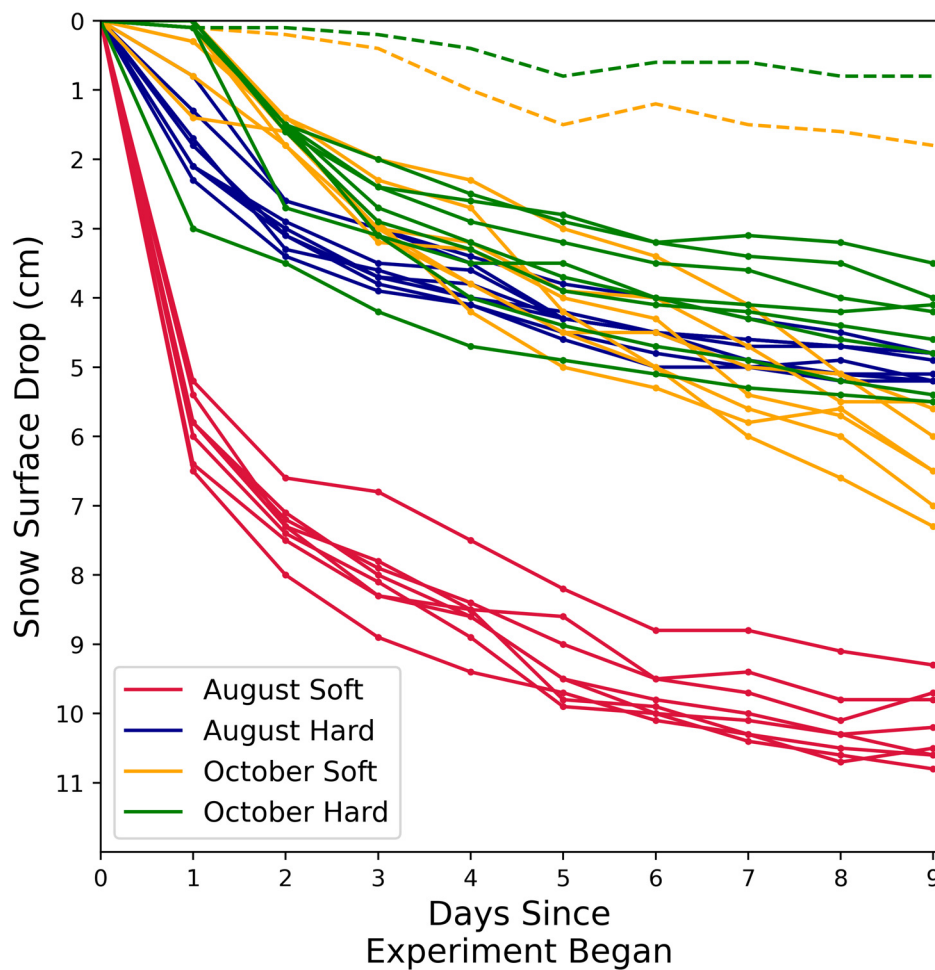


**Figure 6.** The distance descended by the snow surface in all samples, measured from upper rim of the black plastic tube which was the original position of the snow surface when brine was added at the base. The initial sample height was 19 cm. Solid lines indicate brine-wetted samples, dashed lines indicate control samples that were left brine-free during the second round of experiments.

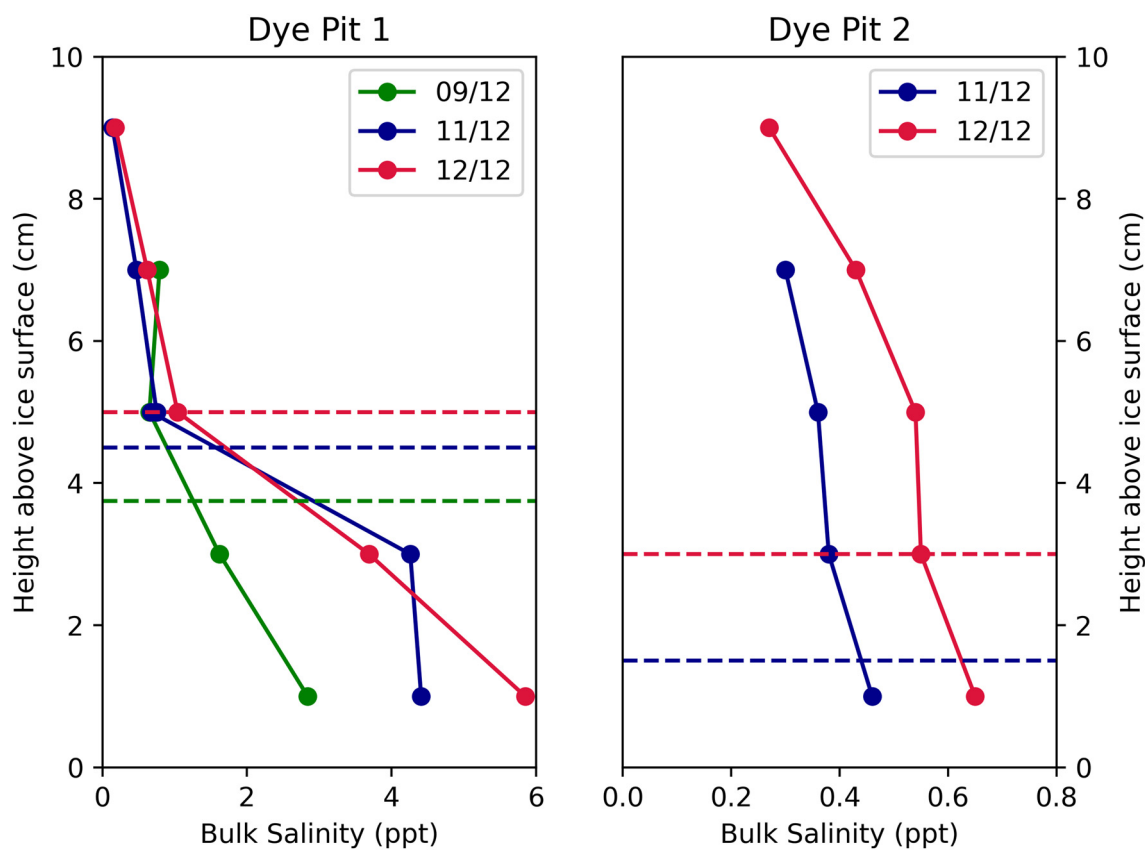


**Figure 7.** Snow salinity profiles for the two sea-ice sites near Churchill on the dates they were visited. Horizontal dashed lines show the height to which dye had migrated by a given date. The height travelled by the dye increased day by day at both pits, as did the snow salinity values.

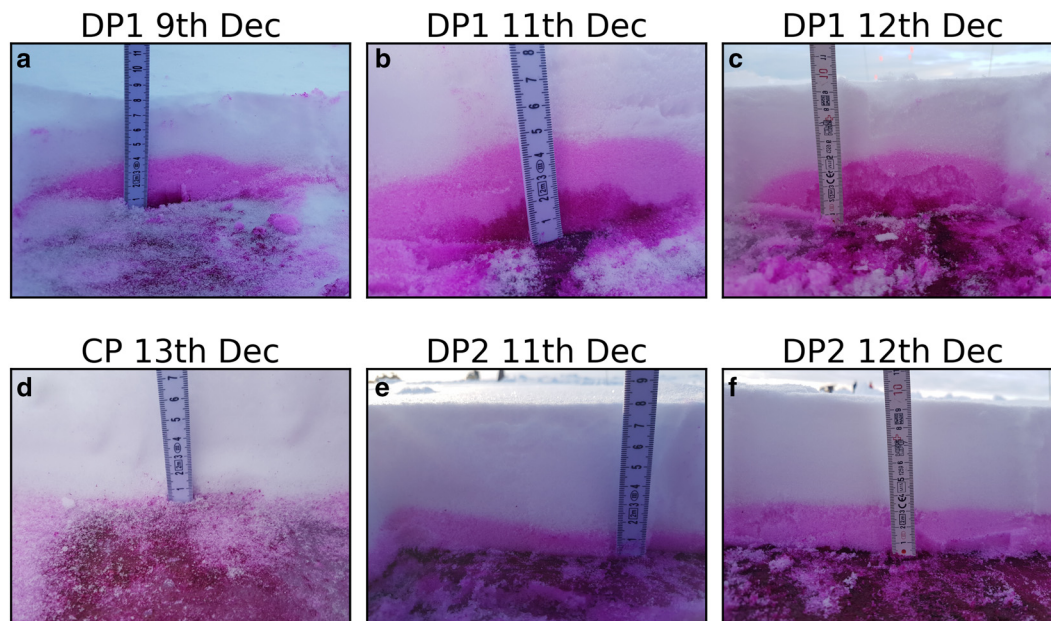


**Figure 8.** Photographs showing the results of the brine wicking experiments (DP Panels) and the control experiment on lake ice (CP). Dye was deployed at DP1 on the 4th December, and at DP2 and CP on the 9th. Upward migration of the dye into the snow is clearly visible over the sea ice, but is not in evidence on the lake ice, where the ice remained strongly dyed but the snow above was not. Significant lateral migration of the dye was visible at DP1 where the dye was originally deployed along a line.

be  $917 \text{ kg m}^{-3}$  (Fukusako, 1990). Based on Eqn (2), the volumetric fractions of air in our four snow layers (August Soft/Hard, October Soft/Hard) are 0.74, 0.59, 0.84 and 0.83. If we then assume that the 50 ml of brine undergoes no dilution instantaneously, we can calculate the fraction of the snow's pore space occupied by considering the wicking heights of the samples and the dimensions of the container. We first note that the pore space available is simply  $P$  multiplied by the volume of snow that experiences wicking. This volume can be expressed as the cross-sectional area of the pipe ( $A$ ) multiplied by the wicking height ( $W_h$ ). The fraction of the original snow pore spaces taken up by the brine ( $F_{\text{pore}}$ ) after wicking is therefore:

$$F_{\text{pore}} = \frac{B_{\text{vol}}}{W_h \times A \times P} \quad (3)$$

Where  $B_{\text{vol}}$  is the volume of added brine (in this case 50 ml),  $W_h$  is the observed wicking height upon immediate dissection,  $A$  is the cross-sectional area of the sample (in this case  $0.031 \text{ m}^2$ ), and  $P$  is the original porosity of the dry snow sample per Eqn (2). Taking the average of the initially checked samples in round 1, we find that the initial fraction of the pore spaces taken up ( $F_{\text{pore}}$ ) are (Aug Soft/Hard, Oct Soft/Hard): 60, 78, 87 and 99%. This is a strikingly large range of values, and the values are not correlated with the SSA or density measurements made on the respective layers.

We might speculate that the fraction of the pore space initially taken up by the brine may reflect the connectivity of the pores for which air-permeability would be a proxy. In the case where pore spaces are highly connected, it is possible that the brine will occupy more of the available air space and thus not wick as high. However, the nature of the ensuing phase equilibrium between the ice and the brine within the snow means that the ice is constantly melting and refreezing; this process would likely transform the microstructure and thus the pore connectivity. If it is indeed the case that the brine initially wicks higher in snow with a higher fraction of isolated pores that cannot be filled with brine, then we might expect that the subsequent microstructural transformation would allow these pores to be filled and suppress subsequent upward wicking. In fact, it does not appear that

the August samples (which experienced higher initial wicking) experienced less upward wicking over time.

We now discuss the strong correlation (but offset values) between the salinity of the released brine and the salinity of the liquid phase in the bulk snow volume above (Fig. 5). First we investigate how the brine compares to the equilibrium brine salinity. To do this we can initially assume that after 9 d we have reached a full phase-equilibrium between the brine and the ice; Eqn (1) indicates that at the temperature of the freezer the equilibrium brine salinity is 94 ppt, which is considerably higher than the brine that was released (values between 50 and 75 ppt). Furthermore, the pink colouring of the immediately dissected samples was much more vivid than in the samples dissected after 9 d, indicating a significant degree of dilution of brine within the sample, beyond what would be expected from a transition of our 100 ppt brine to an equilibrium salinity of 94 ppt. This suggests that Eqn (1) (which was derived from sea-ice observations) may not be fully applicable to the brine-in-snow scenario. It is important to note however that the released brine was often partially frozen in the weighing boat by the time it was removed and measured after 9 d. In this sense, we are measuring the salinity of what may be viewed as a bulk sample, and not the salinity of a purely liquid brine in an equilibrium with unmeasured ice per Eqn (1).

#### 4.2. Churchill field experiments

The evolution of the salinity profiles over sea ice is of interest independently of the dye behaviour. It appears that even in cold conditions ( $< -10^\circ\text{C}$ ; Fig. 2c), accumulating snow on sea ice generates a characteristic monotonic profile, and that this profile can evolve in a matter of days. This is novel, as most studies have looked at increases in snow salinity over new ice in comparatively warm conditions (see Dominé and others, 2004, for discussion of this).

A potential challenge to the above analysis involves the lateral variability in ice surface salinity. One can imagine that as we dug snow pits along the ice over time, we inadvertently sampled increasingly saline ice due to lateral variability which induced increasingly saline snow even in the absence of any time-evolution

of the system. We argue that the *decreasing* ice surface salinity of the DP1 pits over time indicates that this is not the case (with DP2 being relatively inconclusive in this regard).

Turning to the observed dye heights, they increased over time along with the snow salinity values. Although we do not have enough data to investigate whether larger increases in the basal salinity were associated with larger increases in the wicked height, the fact that we saw no dye migration at the lake site where there was no snow salinity is instructive. This suggests that the development of both pits' characteristic monotonic salt profile is at least in part directly driven by upward migration of brine from the ice surface. While some of the salt may be deposited from the atmosphere, or be delivered with the snow that was blown into the trench, there is only one source of dye: the ice surface. For dye to move up into the snow, we conclude it must have migrated upwards from there via a liquid water pathway.

The fact that the dye was able to travel upwards at all in such cold temperatures and low bulk salinities is perhaps surprising, particularly for DP2. Using the bulk salinity of the snow and coincident temperature measurements of the layers, we can estimate the brine volume fraction (BVF) of the snow using Eqn 3 from Frankenstein and Garner (1967):

$$\text{BVF} = S_{\text{bulk}} \left( \frac{45.917}{-T_s} + 0.93 \right) \quad (4)$$

Where  $S_{\text{bulk}}$  and  $T_s$  are the bulk salinity and temperature of the snow layer in question. In order to calculate an upper-bound on the snow BVF, we consider the basal (bottom 2 cm) snow layers of DP1 and DP2, which were consistently the warmest and most saline. At DP1 we calculate increasing BVF values of 1.7, 2.8 and 4.5% on the 9th, 11th and 12th of December respectively (Table 1). At DP2 these values are an order of magnitude lower (due to the much lower bulk salinities), at 0.3 and 0.5% for the 11th and 12th of December, respectively. Given the BVFs are so much lower, it is noteworthy that the dye wicking height is not suppressed by a similar factor.

Work by Denoth (1980) indicates that the transition of fresh liquid water from the pendular to the funicular regime occurs in the range of 11–15% of the pore volume (not the BVF). We can convert BVF values to the fraction of the pore volume filled by calculating the porosity of the basal snow following a version of Eqn (2) modified for the presence of the brine itself, following Section 2.2 of Geldsetzer and others (2009):

$$P = 1 - \frac{\rho_s - (\text{BVF} \times \rho_b)}{\rho_{\text{ice}}} \quad (5)$$

Where all variables have the same definitions as in Eqn (2) and  $\rho_b$  represents the density of the brine, which we calculate using Eqn 16 of Cox and Weeks (1975):

$$\rho_b = 1 + 0.0008S_b \quad (6)$$

**Table 1.** Values used in the calculation of the fraction of the available pore space taken up by brine at DP1 and DP2

Pit	Date	Temperature (°C)	BVF (%)	Density (kg m <sup>-3</sup> )	P	BVF/P (%)
DP1	9 <sup>th</sup> Dec	-8.92	1.73	154	0.83	2.07
DP1	11 <sup>th</sup> Dec	-8.40	2.82	255	0.72	3.91
DP1	12 <sup>th</sup> Dec	-6.86	4.46	223	0.76	5.89
DP2	11 <sup>th</sup> Dec	-7.80	0.31	185	0.80	0.39
DP2	12 <sup>th</sup> Dec	-6.34	0.53	194	0.79	0.67

BVF refers to brine volume fraction per Eqn (4). P refers to porosity per Eqn (5). Values for BVF/P generally do not exceed the threshold for the transition to the funicular regime given by Denoth (1980).

To calculate the fraction of the pore space taken up by the brine, we divide the brine volume fraction (Eqn (4)) by the brine-adjusted porosity (Eqn (5)). Because of the low BVF values we find that adjusting the porosity calculation shown in Eqn (2) for the brine weight does not make a difference to the three significant figures of precision shown in Table 1. In the basal snow layers the fraction of the pore space filled by brine (BVF/P column of Table 1) is generally around 20–40% larger than the brine volume fraction values themselves; the largest values for both pits occur on the 12<sup>th</sup> of December and are 5.8 and 0.67% for DP1 and DP2 respectively (see Table 1). These values are well short of the 11% described by Denoth (1980) for shifting from the pendular to funicular regime. However, we note that those values are for *fresh* water in snow, which may have a different microscopic arrangement due to transformation of the microstructure by the brine. Our results indicate that vertical liquid pathways of several centimetres length do exist from the snow/ice interface into the snow volume, even at low salinity values and temperatures.

One uncertainty in this technique concerns whether the dye always traces the upward flux of brine, or simply illuminates pathways of interconnected brine pockets by diffusion. In the field-work presented here we were able to measure consistently increasing snow salinity so it does appear that the sign of the brine flux was at least positive in the upward direction, even if the magnitude was small at DP2. We do therefore raise the possibility that the presence of salt produced a series of thin, interconnected liquid films through which the dye was able to diffuse in the absence of significant bulk movement of liquid. The control experiment indicates that this is only possible in the presence of salt, and that the snow's inherent quasi-liquid layers are not sufficient for the brine to diffuse if this indeed occurs at all. In the photographs of DP1 presented in Figure 8 there is a visible two-tone pattern of a darker shade of dye below a lighter shade. We were unable to identify a root cause of this pattern, which is not visible at DP2 where the colour was relatively uniform over the dyed area of snow. However, we do note that the ice at DP1 was smoother than the ice at DP2, and the dye was much more abundantly deployed at DP1 because the spray-gun was not used.

Results from DP1 indicate that the dye migrated further horizontally than it did vertically. One simple explanation for this is that the dye moved horizontally through the top layer of the ice (which has a substantial liquid water component even in cold conditions), and then moved vertically up through the snow. However, it is also possible that horizontal migration in the snow is energetically favourable compared to vertical migration because gravity does not act in opposition. If the dye did indeed move substantially through the snow in a lateral direction, it raises questions about the role of snow's microstructural anisotropy in brine/dye wicking. This is of interest when considering the fact that we rotated the snow samples in our laboratory experiments, and dye was wicking against gravity but laterally through the snow with respect to its initial orientation.

### 4.3. Experimental constraints and future directions

Our snow samples in the laboratory were produced by horizontally driving pipes into distinct stratigraphic layers that we observed. We then rotated the pipes so that brine could be introduced at the base, meaning the snow was no longer in the orientation in which it accumulated. If the snow had significant microstructural anisotropy, then this will have diminished the realism of our experiments. Furthermore, if the snow has small-scale vertical layering in situ then that may contribute to horizontal variability in the wicked height once the sample has been rotated. Our results showed that wicking did not exceed 7

cm in height, so our 19 cm sampling tubes were excessively long for this experiment. In future the tubes could potentially be inserted vertically if a homogenous stratigraphic snow layer of sufficient thickness to accommodate the wicking is found. It would also be valuable to study how snow stratigraphy controls brine wicking, as a layered structure is commonly observed in a natural snow-covered sea-ice environment.

Our freezer did not have a reliably adjustable thermostat, so we carried out all our work at a fixed temperature of around  $-5.6^{\circ}\text{C}$ . Furthermore, there was some temperature cycling due to the gas-thermostat's control over the compressor. While the real environment of course features fluctuating air temperature on various timescales, removing the temperature cycling inside the freezer would be desirable as it would simplify the physics. Furthermore, it would be very instructive to perform the same suite of experiments at different temperatures, as this would control the equilibrium salinity and brine volume fraction inside the snow.

We performed our experiment at  $\sim -5.6^{\circ}\text{C}$ , and therefore used a high salinity (100 ppt) brine. While this brine may reflect realistic values for a brine skim formed through upward brine rejection (e.g. Barber and others, 2014, and references therein), it is unrepresentative of the salinity of the seawater that can flood the base of the snowpack. The amount of brine supplied also exceeds that which would be supplied by a brine skim. Future research on brine-wicking after flooding should therefore aim to use a more appropriate brine salinity when used in this quantity. This would require careful operation at a higher temperature to allow the brine to be added at the same temperature as the snow.

We were only able to characterise the snow microstructure using the snow micropenetrator, and we have assumed that its sampling of the snow layers from which the samples were taken accurately reflects the snow samples themselves. This may not be the case, especially if the snow samples undergo microstructural metamorphosis inside the freezer. To investigate the potential for this, we first attempted to drive the SMP through the snow samples in their tubes; we found that due to the conical shape of the probe, snow was forced against the sides of the tube and readings were unreliable.

We also measured the degree of settling of two dummy samples (one from hard snow, and one from soft snow) which did not have brine added to them during the second round of experiments. We found that over the 9 d, the soft snow sank 1.8 cm into the tube, and the hard snow sank 0.8 mm. Assuming the mass of snow was conserved, this corresponds to an increase in the density of the snow samples of 9.4 and 4.2% respectively. This densification is likely caused by microstructural change, and this would ideally be monitored with a method such as micro-CT scanning in future. However, we did not quantify the role of snow sublimation over the experiment. As well as affecting the densification, sublimation may also have changed the microstructure from that which was measured by the SMP. Sublimation could be monitored in future by weighing the samples at regular intervals during the experiment, and noting any reductions in mass. Furthermore, the downward release of brine later in the experiments could be contextualised with additional data collection in future experiments. In particular, the evolution of the salt distribution at higher temperatures (similar to the summer melt) could be monitored, rather than ending the experiment abruptly. Any future changes in the experimental setup should be accompanied by similar changes to the reference samples that measure the rate at which dry, fresh snow settles.

As for the brine-filled samples, micro-CT scanning may be able to resolve the exact microstructural configuration of the snow after being in contact with the brine. It also has the potential

to image exactly how much of the pore volume remains available both after initial wicking and after 9 d. Furthermore, it could resolve the previously posed questions regarding the original connectivity of the pore structures in the snow. Finally, and most critically, micro-CT scanning is a non-destructive technique which sharply contrasts with our dissection-based approach. With an appropriate contrast medium, the technology may allow monitoring of the migration of brine up a sample over time without destroying it, even with low-resolution CT-scanning technology available in the medical sector (as opposed to micro-CT technology often applied in research). Such technology at any resolution would also shed light on the internal homogeneity of the samples within the tubes.

#### 4.4. Field constraints and future directions

Sea ice can generally only be travelled upon when the ice is thick enough to support humans. By the time this is the case and the weather conditions are suitable, it has often already accumulated snow and/or frost flowers. To place dye on the ice surface before snow falls on it would likely either require the use of a small boat, or opportunistic sampling of a newly refrozen lead from thicker ice at its edge. An alternative would be the use of an artificial sea-ice mesocosm (sometimes referred to as a *sea-ice tank*). These facilities often feature gantries from which dye could be applied in the early stages of sea-ice formation.

The means by which the dye was applied to the sea-ice surface could be improved relative to the setup reported here. For both the lab and the field experiments, the quantity of the dye deployed was not controlled, so perceived dilution later could only be qualitatively identified. Furthermore, the application with the spray-gun was patchy rather than even. In future, low volume spray nozzles could be used to apply dye evenly. We stress that our field results are limited to two sites near Churchill, which while cold, is at a latitude of  $58.8^{\circ}\text{N}$  with a nearby river outlet that potentially changes the ice properties such as structure and salinity. To fully understand brine dynamics in snow on sea ice, further experiments should be conducted with a variety of snow and sea-ice types and morphologies, outside the Hudson Bay. We also stress that our field study was performed in a positive freeboard scenario, and therefore does not represent the case of negative freeboard and ice flooding which may well be more common in Antarctica (among other differences). Finally, our field investigation was carried out shortly after freeze-up over a relatively short timescale compared to the length of the October–April cold season. Future experiments should therefore focus on longer timescales to capture seasonal effects, perhaps even continuing into the summer melt.

Despite the above limitations, our field results from Churchill have several implications: the first is that the fresher ice surface (DP2) was associated with fresher basal snow. This suggests that the bulk ice surface salinity is a control on the salinity of the underlying snow, but that the control is non-linear given that the basal snow was ten times fresher in response to a fresher ice surface by a factor of only three. Relatedly, this suggests that the conditions in which the ice freezes up may impact the subsequent overlying snow salinity. The snow developed its characteristic monotonic vertical salinity profile, and supported dye migration at low temperatures ( $< -10^{\circ}\text{C}$ ). This implies that this vertical profile is potentially widespread over FYI, and is not dependent on warm conditions to increase the snow brine volume fraction above 5%.

## 5. Summary

We have presented results from lab and field experiments using rhodamine-WT dye to trace the upward movement of brine in

snow. Our lab experiments differed from the field because we actively supplied brine alongside the dye, leading to a larger initial volume of liquid in the snow, with commensurately higher bulk salinities. Despite their differences, both settings exhibited obvious upward migration of the dyed brine, indicating that the phenomenon occurs in comparatively dry and wet snow regimes.

Our results are not trivial to interpret. This is particularly the case in the lab, where snow density and SSA estimates did not appear to be related to the height to which the dye wicked, either initially or on a multi-day timescale. Despite brine being added to the snow base at close to its equilibrium salinity, a more diluted brine was released from the base of the samples after several days. We attribute the rejection to salinity-driven microstructural metamorphosis which made the snow less capable of holding liquid.

Our control experiment from the field indicated that saline ice was required for the dye to migrate upwards. The dye migrated several centimetres up into the snow even when snow salinity measurements implied that <1% of the pore space was occupied by brine; the exact way in which this occurred remains unknown, but could be resolved in future with micro-CT imaging.

**Supplementary material.** The supplementary material for this article can be found at <https://doi.org/10.1017/aog.2024.27>.

**Data.** Analysis code, figure files and underlying data are available at: [https://github.com/robbiemallett/dye\\_brine](https://github.com/robbiemallett/dye_brine). This information has been persistently archived at: <https://doi.org/10.5281/zenodo.11387505>

**Acknowledgements.** This work was funded in part by the Canada 150 Research Chairs Programme (Grant #50296), providing funding for R. M., V. N., J. S., R. W. and M. S. R. M. was additionally supported by the NERC Doctoral Training Partnership (NE/L002485/1) during the field experiments in Churchill, while R. M., J. S., R. W., G. V. and J. W. also received funding from the NERC DEFIANT grant (NE/W004739/1) in support of data collection and analysis at Rothera Station. R. W. and J. S. also received funding from the European Union's Horizon 2020 research and innovation programme via project CRiceS (Grant 101003826) and from the European Space Agency NEOMI grant 4000139243/22/NL/SD. R. M. would also like to acknowledge funding and support from the International Space Science Institute (Team no. 510). The authors would like to thank the wintering staff of Rothera Research Station, and Brian Gullick at the Churchill Northern Studies Centre for facilitating this research.

**Author contributions.** R. M. and V. N. conceived the protocols, led the field study and performed the lab work at Rothera research station. R. W., J. S., J. Y. and M. S. contributed to the Churchill field campaign, including gathering the snow pit data and analysing snow samples. J. W. and G. V. contributed feedback and conceptualisation of the lab study. All authors contributed to the final manuscript.

## References

- Babb DG and 8 others** (2023) The stepwise reduction of multiyear sea ice area in the Arctic Ocean since 1980. *Journal of Geophysical Research: Oceans* **128**(10), e2023JC020157. doi: [10.1029/2023JC020157](https://doi.org/10.1029/2023JC020157)
- Barber DG and Nghiem SV** (1999) The role of snow on the thermal dependence of microwave backscatter over sea ice. *Journal of Geophysical Research: Oceans* **104**(C11), 25789–25803. doi: [10.1029/1999JC900181](https://doi.org/10.1029/1999JC900181)
- Barber DG and 7 others** (1998) The role of snow on microwave emission and scattering over first-year sea ice. *IEEE Transactions on Geoscience and Remote Sensing* **36**(52), 1750–1763. doi: [10.1109/36.718643](https://doi.org/10.1109/36.718643)
- Barber DG, Iacozza J and Walker AE** (2003) Estimation of snow water equivalent using microwave radiometry over Arctic first-year sea ice. *Hydrological Processes* **17**(17), 3503–3517. doi: [10.1002/hyp.1305](https://doi.org/10.1002/hyp.1305)
- Barber DG and 8 others** (2014) Frost flowers on young Arctic sea ice: the climatic, chemical, and microbial significance of an emerging ice type. *Journal of Geophysical Research: Atmospheres* **119**(20), 593–11. doi: [10.1002/2014JD021736](https://doi.org/10.1002/2014JD021736)
- Bennington KO** (1967) Desalination features in natural sea ice. *Journal of Glaciology* **6**(48), 845–857. doi: [10.3189/s0022143000020153](https://doi.org/10.3189/s0022143000020153)
- Bernard A, Hagenmuller P, Montagnat M and Chambon G** (2023) Disentangling creep and isothermal metamorphism during snow settlement with X-ray tomography. *Journal of Glaciology* **69**(276), 899–910. doi: [10.1017/JOG.2022.109](https://doi.org/10.1017/JOG.2022.109)
- Butler BM, Papadimitriou S, Santoro A and Kennedy H** (2016) Mirabilite solubility in equilibrium sea ice brines. *Geochimica et Cosmochimica Acta* **182**, 40–54. doi: [10.1016/j.gca.2016.03.008](https://doi.org/10.1016/j.gca.2016.03.008)
- Confer KL and 7 others** (2023) Impact of changing Arctic sea ice extent, sea ice age, and snow depth on sea salt aerosol from blowing snow and the open ocean for 1980–2017. *Journal of Geophysical Research: Atmospheres* **128**(3), e2022JD037667. doi: [10.1029/2022JD037667](https://doi.org/10.1029/2022JD037667)
- Cox GF and Weeks WF** (1975) Brine drainage and initial salt entrapment in sodium chloride ice. *US Army Corps of Engineers Cold Regions Research and Engineering Laboratory Research Report*, 345.
- Crocker GB** (1984) A physical model for predicting the thermal conductivity of brine-wetted snow. *Cold Regions Science and Technology* **10**(1), 69–74. doi: [10.1016/0165-232X\(84\)90034-X](https://doi.org/10.1016/0165-232X(84)90034-X)
- Davis RE and Dozier J** (1984) Snow wetness measurement by fluorescent dye dilution. *Journal of Glaciology* **30**(106), 362–363. doi: [10.3189/S0022143000006225](https://doi.org/10.3189/S0022143000006225)
- Denoth A** (1980) The pendular-funicular liquid transition in snow. *Journal of Glaciology* **25**(91), 93–98. doi: [10.3189/S0022143000010315](https://doi.org/10.3189/S0022143000010315)
- Dominé F and Shepson PB** (2002) Air-snow interactions and atmospheric chemistry. *Science* **297**(5586), 1506–1510. doi: [10.1126/SCIENCE.1074610/ASSET/D6C41CA3-8555-4C68-BB61-9BAE445F0944/ASSETS/G-RAPHIC/SE3420818004.JPEG](https://doi.org/10.1126/SCIENCE.1074610/ASSET/D6C41CA3-8555-4C68-BB61-9BAE445F0944/ASSETS/G-RAPHIC/SE3420818004.JPEG)
- Dominé F, Sparapani R, Ianniello A and Beine HJ** (2004) The origin of sea salt in snow on Arctic sea ice and in coastal regions. *Atmospheric Chemistry and Physics Discussions* **4**(4), 4737–4776. doi: [10.5194/acpd-4-4737-2004](https://doi.org/10.5194/acpd-4-4737-2004)
- Drinkwater MR and Crocker GB** (1988) Modelling changes in the dielectric and scattering properties of young snow-covered sea ice at GHz frequencies. *Journal of Glaciology* **34**(118), 274–282. doi: [10.3189/s0022143000007012](https://doi.org/10.3189/s0022143000007012)
- Eide LI and Martin S** (1975) The formation of brine drainage features in young sea ice. *Journal of Glaciology* **14**(70), 137–154. doi: [10.3189/S0022143000013460](https://doi.org/10.3189/S0022143000013460)
- Essery R, Morin S, Lejeune Y and B Ménard C** (2013) A comparison of 1701 snow models using observations from an Alpine site. *Advances in Water Resources* **55**, 131–148. doi: [10.1016/j.advwatres.2012.07.013](https://doi.org/10.1016/j.advwatres.2012.07.013)
- Frankenstein G and Garner R** (1967) Equations for determining the brine volume of sea ice from  $-0.5^{\circ}\text{C}$  to  $-22.9^{\circ}\text{C}$ . *Journal of Glaciology* **6**(48), 943–944. doi: [10.3189/S0022143000020244](https://doi.org/10.3189/S0022143000020244)
- Freitag J and Eicken H** (2003) Meltwater circulation and permeability of Arctic summer sea ice derived from hydrological field experiments. *Journal of Glaciology* **49**(166), 349–358. doi: [10.3189/172756503781830601](https://doi.org/10.3189/172756503781830601)
- Frey MM and 9 others** (2020) First direct observation of sea salt aerosol production from blowing snow above sea ice. *Atmospheric Chemistry and Physics* **20**(4), 2549–2578. doi: [10.5194/ACP-20-2549-2020](https://doi.org/10.5194/ACP-20-2549-2020)
- Fukusako S** (1990) Thermophysical properties of ice, snow, and sea ice. *International Journal of Thermophysics* **11**(2), 353–372. doi: [10.1007/BF01133567](https://doi.org/10.1007/BF01133567)
- Geldsetzer T, Langlois A and Yackel J** (2009) Dielectric properties of brine-wetted snow on first-year sea ice. *Cold Regions Science and Technology* **58**(1-2), 47–56. doi: [10.1016/j.coldregions.2009.03.009](https://doi.org/10.1016/j.coldregions.2009.03.009)
- Gong X and 18 others** (2023) Arctic warming by abundant fine sea salt aerosols from blowing snow. *Nature Geoscience* **2023** **16**(9), 768–774. doi: [10.1038/s41561-023-01254-8](https://doi.org/10.1038/s41561-023-01254-8)
- Industrial Process Measurement Inc** (2016) Water quality meters; Oakton Waterproof pH 450, CON 450 and pH/CON 450 Meters. Technical report, <https://www.instrumentation2000.com/media/pdf/oakton-ph-con-450-datasheet.pdf>.
- Liston GE and 7 others** (2020) A Lagrangian snow-evolution system for sea-ice applications (snowmodel-LG): part I – model description. *Journal of Geophysical Research: Oceans* **125**(10), e2019JC015913. doi: [10.1029/2019jc015913](https://doi.org/10.1029/2019jc015913)
- Markus T, Stroeve JC and Miller J** (2009) Recent changes in Arctic sea ice melt onset, freezeup, and melt season length. *Journal of Geophysical Research: Oceans* **114**, C12024. doi: [10.1029/2009JC005436](https://doi.org/10.1029/2009JC005436)
- Massom RA and 13 others** (2001) Snow on Antarctic sea ice. *Reviews of Geophysics* **39**(3), 413–445. doi: [10.1029/2000RG000085](https://doi.org/10.1029/2000RG000085)
- Nandan V and 7 others** (2016) Ku-, X- and C-band measured and modeled microwave backscatter from a highly saline snow cover on

- first-year sea ice. *Remote Sensing of Environment* **187**, 62–75. doi: [10.1016/J.RSE.2016.10.004](https://doi.org/10.1016/J.RSE.2016.10.004)
- Nandan V and 8 others** (2017) Effect of snow salinity on CryoSat-2 Arctic first-year sea ice freeboard measurements. *Geophysical Research Letters* **44**(20), 419–426. doi: [10.1002/2017GL074506](https://doi.org/10.1002/2017GL074506)
- Nandan V and 12 others** (2020) Snow property controls on modeled Ku-band altimeter estimates of first-year sea ice thickness: case studies from the Canadian and Norwegian Arctic. *IEEE Journal of Selected Topics in Applied Earth Observations and Remote Sensing* **13**, 1082–1096. doi: [10.1109/JSTARS.2020.2966432](https://doi.org/10.1109/JSTARS.2020.2966432)
- Nicolaus M, Haas C and Willmes S** (2009) Evolution of first-year and second-year snow properties on sea ice in the Weddell Sea during spring-summer transition. *Journal of Geophysical Research Atmospheres* **114**(17), D17109. doi: [10.1029/2008JD011227](https://doi.org/10.1029/2008JD011227)
- Perovich DK and Richter-Menge JA** (1994) Surface characteristics of lead ice. *Journal of Geophysical Research: Oceans* **99**(C8), 16341–16350. doi: [10.1029/94JC01194](https://doi.org/10.1029/94JC01194)
- Petty AA, Webster M, Boisvert L and Markus T** (2018) The NASA Eulerian Snow On Sea Ice Model (NESOSIM) v1.0: initial model development and analysis. *Geoscientific Model Development* **11**(11), 4577–4602. doi: [10.5194/gmd-11-4577-2018](https://doi.org/10.5194/gmd-11-4577-2018)
- Proksch M, Löwe H and Schneebeli M** (2015a) Density, specific surface area, and correlation length of snow measured by high-resolution penetrometry. *Journal of Geophysical Research: Earth Surface* **120**(2), 346–362. doi: [10.1002/2014JF003266](https://doi.org/10.1002/2014JF003266)
- Proksch M and 6 others** (2015b) MEMLS3&a: microwave emission model of layered snowpacks adapted to include backscattering. *Geoscientific Model Development* **8**(8), 2611–2626. doi: [10.5194/gmd-8-2611-2015](https://doi.org/10.5194/gmd-8-2611-2015)
- Proksch M, Rutter N, Fierz C and Schneebeli M** (2016) Intercomparison of snow density measurements: bias, precision, and vertical resolution. *Cryosphere* **10**(1), 371–384. doi: [10.5194/TC-10-371-2016](https://doi.org/10.5194/TC-10-371-2016)
- Provost C and 7 others** (2017) Observations of flooding and snow-ice formation in a thinner Arctic sea-ice regime during the N-ICE2015 campaign: influence of basal ice melt and storms. *Journal of Geophysical Research: Oceans* **122**(9), 7115–7134. doi: [10.1002/2016JC012011](https://doi.org/10.1002/2016JC012011)
- Sazaki G, Zepeda S, Nakatsubo S, Yokomine M and Furukawa Y** (2012) Quasi-liquid layers on ice crystal surfaces are made up of two different phases. *Proceedings of the National Academy of Sciences of the United States of America* **109**(4), 1052–1055. doi: [10.1073/PNAS.1116685109/SUPPL\\_FILE/SM04.AVI](https://doi.org/10.1073/PNAS.1116685109/SUPPL_FILE/SM04.AVI)
- Schneebeli M and Johnson JB** (1998) A constant-speed penetrometer for high-resolution snow stratigraphy. *Annals of Glaciology* **26**, 107–111. doi: [10.3189/1998AOG26-1-107-111](https://doi.org/10.3189/1998AOG26-1-107-111)
- Smart PL and Laidlaw IM** (1977) An evaluation of some fluorescent dyes for water tracing. *Water Resources Research* **13**(1), 15–33. doi: [10.1029/WR013I001P00015](https://doi.org/10.1029/WR013I001P00015)
- Stogryn A** (1986) A study of the microwave brightness temperature of snow from the point of view of strong fluctuation theory. *IEEE Transactions on Geoscience and Remote Sensing* **GE-24**(2), 220–231. doi: [10.1109/TGRS.1986.289641](https://doi.org/10.1109/TGRS.1986.289641)
- Stroeve J and Notz D** (2018) Changing state of Arctic sea ice across all seasons. *Environmental Research Letters* **13**(10), 103001. doi: [10.1088/1748-9326/aade56](https://doi.org/10.1088/1748-9326/aade56)
- Weeks W** (1968) Understanding the variations of the physical properties of sea ice. In *SCAR/SCOR/ IAP0jiUPS Symposium on Antarctic Oceanography (Santiago, Chile, 1966)*, 173–190, SCAR/SCOR/ IAP0jiUPS Symposium on Antarctic Oceanography (Santiago, Chile, 1966), Cambridge, England: Scott Polar Research Institute.
- Wever N and 6 others** (2020) Version 1 of a sea ice module for the physics-based, detailed, multi-layer SNOWPACK model. *Geoscientific Model Development* **13**(1), 99–119. doi: [10.5194/gmd-13-99-2020](https://doi.org/10.5194/gmd-13-99-2020)
- Willatt RC, Giles KA, Laxon SW, Stone-Drake L and Worby AP** (2010) Field investigations of Ku-band radar penetration into snow cover on Antarctic sea ice. *IEEE Transactions on Geoscience and Remote Sensing* **48**(1), 365–372. doi: [10.1109/TGRS.2009.2028237](https://doi.org/10.1109/TGRS.2009.2028237)
- Wren SN, Donaldson DJ and Abbatt JP** (2013) Photochemical chlorine and bromine activation from artificial saline snow. *Atmospheric Chemistry and Physics* **13**(19), 9789–9800. doi: [10.5194/ACP-13-9789-2013](https://doi.org/10.5194/ACP-13-9789-2013)
- Yackel J and 6 others** (2019) Snow thickness estimation on first-year sea ice from late winter spaceborne scatterometer backscatter variance. *Remote Sensing* **11**(4), 417. doi: [10.3390/rs11040417](https://doi.org/10.3390/rs11040417)